Effects of Excluded Volume upon Protein Stability in Covalently Cross-Linked Proteins with Variable Linker Lengths[†]

Yun Ho Kim[‡] and Wesley E. Stites*

Department of Chemistry and Biochemistry, University of Arkansas, Fayetteville, Arkansas 72701-1021

Received February 20, 2008; Revised Manuscript Received May 24, 2008

ABSTRACT: To explore the effects of molecular crowding and excluded volume upon protein stability, we used a series of cross-linking reagents with nine different single-cysteine mutants of staphylococcal nuclease to make covalently linked dimers. These cross-linkers ranged in length from 10.5 to 21.3 Å, compelling separations which would normally be found only in the most concentrated protein solutions. The stabilities of the dimeric proteins and monomeric controls were determined by guanidine hydrochloride and thermal denaturation. Dimers with short linkers tend to exhibit pronounced three-state denaturation behavior, as opposed to the two-state behavior of the monomeric controls. Increasing linker length leads to less pronounced three-state behavior. The three-state behavior is interpreted in a three-state model where cross-linked native protein dimer, N−N, interconverts in a two-state transition with a dimer where one protein subunit is denatured, N−D. The remaining native protein in turn can denature in another two-state transition to a state, D−D, in which both tethered proteins are denatured. Three-state behavior is best explained by excluded volume effects in the denatured state. For many dimers, linkers longer than 17 Å removed most three-state character. This sets a limit on the flexibility and size of the denatured state. Notably, in contradiction to theoretical predictions, these cross-linked dimers were not stabilized. The failure of these predictions is possibly due to neglect of the alteration in hydrophobic exposure that accompanies any significant reduction in the conformational space of the denatured state.

Levels of macromolecules are very high in vivo compared to the very dilute macromolecular concentrations commonly used in vitro (*1*). This property of cells, often termed molecular crowding, has been recognized for some time (*1, 2*), but more recently the question of how molecular crowding alters protein stability and association has attracted more widespread attention (*3–9*).

Macromolecules are, of course, relatively large molecules. Inside a typical cell they occupy some 20−30% of the space (*5, 10, 11*). The concentration of any one species is relatively low; hence, the term "concentrated" is generally avoided in favor of "crowded", but regardless of the terminology, it is obvious that conditions are far from the condition of infinite dilution where a protein folds and unfolds in isolation.

Our interest here is addressing the impact of such conditions upon protein stability. Protein stability is the free energy difference between the relatively compact and ordered native state and the disordered and relatively expanded denatured state. It is well accepted that the principal driving force for unfolding is entropy (*12*). The denatured state has much more conformational entropy than the native state. In the absence of attractive or repulsive intramolecular interactions, excluded volume should conformationally limit the denatured state and hence destabilize it, thus increasing protein stability. The theory for this effect is well-developed (*10, 13–18*).

However, there is not a great deal of experimental evidence about this issue. Monitoring the effect upon one particular relatively dilute protein species in a complex soup of other proteins present in large amounts presents obvious experimental difficulties. Eggers and Valentine (*19*) used another method to prevent this problem, mimicking the effects of confinement and crowding on the structure and stability of proteins by enclosing the proteins within the pores of sol−gel glass. They found that this increased the melting temperature of α-lactalbumin by as much as 32 °C. On the other hand, other proteins did not exhibit any increase in stability. Similarly, Flaugh and Lumb (*20*) tested the hypothesis that the intrinsically disordered proteins c-Fos and $p27^{Kip1}$ would adopt folded structures under crowded conditions in which excluded volume is predicted to stabilize compact, native conformations. Using dextrans and Ficoll to provide molecular crowding effects, they found no induced ordered structure in these normally disordered proteins. Similarly, the stability of FK-506-binding protein was found to be minimally affected by Ficoll (*21*).

Aside from the sparse number of studies addressing this issue, there is an important question about such work. The physiological relevance of dextran, Ficoll, and, especially, silica glass is unclear. Further, the size and shape of the pores in a glass are to some degree heterogeneous and uncertain.

Previous work by our research group has been aimed at addressing precisely this issue of excluded volume. We used

[†] This research was supported by NIH Grant NCRR COBRE 1 P20 RR15569.

* To whom correspondence should be addressed. Telephone: (479) 575-7478. Fax: (479) 575-4049. E-mail: wstites@uark.edu.

[‡] Present address: Department of Physical Sciences, Station 23, The University of West Alabama, Livingston, AL 35470-2099.

10.1021/bi800297j CCC: $40.75
Published on Web 07/26/2008

the strategy of introducing intramolecular cross-links into the model protein, staphylococcal nuclease, using the cysteine specific cross-linking reagent 1,6-bismaleimidohexane (BMH)[1] (*22*). There are no cysteines in wild-type staphylococcal nuclease, so single-cysteine substitutions were engineered onto the protein surface providing specific sites for alkylation with cross-linking reagent. After cross-linking, the covalent dimers were purified. Covalent linkage restrains the two proteins at a comparatively well-defined distance and orientation.

Guanidine hydrochloride (GuHCl) denaturation of the crossed-linked dimers showed biphasic unfolding behavior that did not fit the two-state model of unfolding. These cross-linked dimers were fitted to a three-state thermodynamic model [both monomer subunits in the native state (N−N), one monomer subunit native and one denatured (N−D), and both monomer subunits denatured (D−D)] of two unfolding transitions in which the individual subunits cooperatively unfold. These two unfolding transitions were very different from the unfolding of the monomeric protein.

These differences in unfolding behavior were attributed in large part to changes in the denatured state, changes which are thought to be due to the exclusion of nearby volume by the other half of the dimer. If this interpretation is correct, it is direct evidence that excluded volume effects in crowded protein solutions are significant. However, it is important to note that, in contrast to theoretical predictions, we did not observe increases in protein stability. Indeed, the stability of the dimers was usually significantly lowered relative to those of monomers. Some of this appears to be native state effects, but we argued that reducing the volume accessible to the denatured state also reduced hydrophobic exposure and hence stabilized the denatured state, an effect neglected in theoretical treatments.

The cross-linked dimers were also thermally unfolded. In contrast to the GuHCl denaturations, thermal denaturation fitted well to a two-state model, but with greatly elevated van't Hoff enthalpies in many cases. These changes in thermal denaturation that fit a two-state model can be rationalized by hydrophobic interactions in the denatured states as well.

This previous work used only one length of cross-linker. We felt an obvious and useful extension would be to see how the effects of cross-linking varied with linker length. Accordingly, in this study, we have synthesized four different length bismaleimide cross-linkers, related to the BMH used in our first study, and three different length haloacetamide cross-linkers. Using the same nine cysteine mutants of staphylococcal nuclease as before (G29C, G50C, E57C, A60C, K70C, K78C, R105C, A112C, and K134C), we have found very clear and interesting trends as the length of the tether linking the two protein molecules increases.

EXPERIMENTAL PROCEDURES

Protein Expression and Purification. The wild type and all nine single-cysteine mutants of the model protein, staphylococcal nuclease, were prepared as previously described (*22, 23*).

Synthesis of Cross-Linkers. Details of the synthesis of the cross-linkers are available as Supporting Information. The identity of all cross-linkers was verified by ^{1}H NMR (Bruker, 300 MHz), and purity was confirmed by analytical reverse phase HPLC using a Waters 600E system with a 991 photodiode array detector. Single peaks, monitored at 215 nm, free of precursors, were found for all cross-linkers.

Cross-Linking Reaction. Each linker was dissolved in DMSO to make a 15 mM stock solution. Nine different single-cysteine mutants, substituted at glycine 29 or 50 (G29C or G50C, respectively), glutamate 57 (E57C), alanine 60 or 112 (A60C or A112C, respectively), lysine 70, 78, or 134 (K70C, K78C, or K134C, respectively), and arginine 105 (R105C), were used, as well as a wild-type control. Wild-type staphylococcal nuclease has no cysteines and a molecular mass of 16843 Da. All proteins were employed in the cross-linking reaction at a concentration of 10.5 mg/mL (623 μM).

Typically, 10 mg (952 μL, 593 nmol) of purified cysteine mutant or wild type was treated with 1 equiv of bismaleimides (**1**−**4**) or bishaloacetamide (**5**−**12**) in 25 mM sodium phosphate and 100 mM NaCl (pH 7.0). Each cross-linker (19.8 μL, 297 nmol) was added (1:2 cross-linker:protein molar ratio) as a 15 mM solution in DMSO. The reactions were carried out in four-dram borosilicate vials at room temperature for 6 h while being agitated with "flea" stir bars. To the reaction mixture was added 3 volumes of cold ethanol, and the mixture was incubated at −20 °C for 30 min. The precipitate was then spun at 14K rpm in a refrigerated microcentrifuge for 10 min at 4 °C. After the supernatany had been discarded, the resulting pellet was resuspended in 1 mL of denaturing and reducing buffer [25 mM sodium phosphate, 100 mM NaCl, 2 M guanidine hydrochloride, and 10 mM β-mercaptoethanol (2-thioethanol, BME) (pH 7.0)].

Separation of Protein Dimers and Monomers. The crude protein was purified using a Water 600e HPLC system equipped with a Pharmacia Superdex 16/60 gel filtration column using a denaturing and reducing buffer [25 mM sodium phosphate, 100 mM NaCl, 2 M guanidine hydrochloride, and 10 mM BME (pH 7.0)] while being monitored with a photodiode array detector. Integration was performed at 280 nm. Complete baseline resolution was not achieved, although it was sufficient for peak integration and determination of relative dimer yields. Collected dimer fractions, cut conservatively from the front of the peak, were combined, concentrated using a Centricon filter unit to approximately 2 mg/mL, and repurified under the same conditions. The final repurified dimer fractions were combined, concentrated using a Centricon filter unit to approximately 1 mg/mL, and dialyzed twice against 25 mM sodium phosphate and 100 mM NaCl (pH 7.0). Injection of analytical amounts confirmed the absence of monomeric protein.

Ellman's Assay. All purified cross-linked dimers using bismaleimide ($n = 0-3$) and haloacetamide ($n = 0-2$) cross-linkers and modified monomeric controls made using *N*-(2-hydroxyethyl)maleimide (HEM) and 2-bromo-*N*-(2-hydroxyethyl)acetamide (BHA) were subjected to a standard Ellman's assay (*24*) to quantify the extent of reaction at cysteine residues. Wild-type and unreacted cysteine mutants were also assayed as controls.

[1] Abbreviations: BMH, 1,6-bismaleimidohexane; GuHCl, guanidine hydrochloride; BME, β-mercaptoethanol; HEM, *N*-(2-hydroxyethyl-)maleimide; BHA, 2-bromo-*N*-(2-hydroxyethyl)acetamide; TCEP, tricarboxyethylphosphine.

Solvent Denaturations. In general, guanidine hydrochloride (GuHCl) denaturation, followed by fluorescence, were carried out as described previously (*25, 26*). Tricarboxyethylphosphine (TCEP, 0.5 mM) was added to proteins with free thiols to prevent disulfide formation. In one change from our usual procedure, the denaturations were carried out at both the usual 100 and 250 mM sodium chloride. Data analysis using a two-state model was carried out as previously described (*25*). The denaturation data for all cross-linked dimers were also analyzed with a three-state thermodynamic unfolding model previously described (*22*).

Thermal Denaturations. Thermal denaturations, followed by fluorescence, and data analysis were performed as previously described (*22*).

Molecular Modeling. To estimate the maximum sulfur−sulfur distance of each cross-linker, we used the Hyperchem 7 Molecular Modeling program (Hypercube Inc.) to optimize each cross-linker, modified with methyl thiol, in an extended conformation. Various stereochemistries and orientations of the two sulfur-modified reactive groups were modeled to determine which gave the maximal separation.

RESULTS

Cross-Linking. Detailed results of the yields of each cross-linking reaction and of the Ellman's assay confirming that the cross-linking reaction blocked all free cysteines, leading to a dimeric product with defined points of covalent attachment, are available as Supporting Information.

Guanidine Hydrochloride Denaturations. The stability to reversible solvent denaturation of all purified dimers, unreacted monomers, and monomers reacted with monofunctional controls was characterized by fluorescence spectroscopy. Nuclease possesses a single tryptophan located at position 140 which can act as a sensitive probe of structure to distinguish whether the protein molecule is folded or unfolded. Normally, the staphylococcal nuclease and its mutants have very well-behaved denaturations, with a clear sigmoidal curve with relatively flat native and denatured baselines. We noted a tendency for the dimeric proteins to have native baselines with pronounced curvature, which greatly complicates data analysis. For reasons that are not clear to us, such behavior was not as noticeable in our previous BMH cross-linking work. The possibility that this was due to electrostatic interactions in the native state was considered, and therefore, denaturations of the bismaleimide cross-linked dimers were also carried out at an ionic strength higher than normal (250 mM NaCl instead of 100 mM NaCl). At higher ionic strengths, the baseline curvature was significantly reduced in all cases. The titrations of the haloacetamide cross-linked dimers were carried out only at 250 mM NaCl. The titration behavior of representative cross-linked dimers at both ionic strengths is shown in Figure 1.

Analysis of guanidine hydrochloride (GuHCl) denaturations in terms of a simple two-state model yields three parameters: a protein's stability to reversible denaturation in the absence of denaturant (ΔG_{H_2O}), the rate of change of free energy with respect to GuHCl concentration [m_{GuHCl} or d(ΔG)/d[GuHCl]], and the concentration of guanidine hydrochloride at which half the protein molecules are denatured (C_m). These parameters are listed in Table 1 for the unmodified cysteine mutants and wild type, and for these

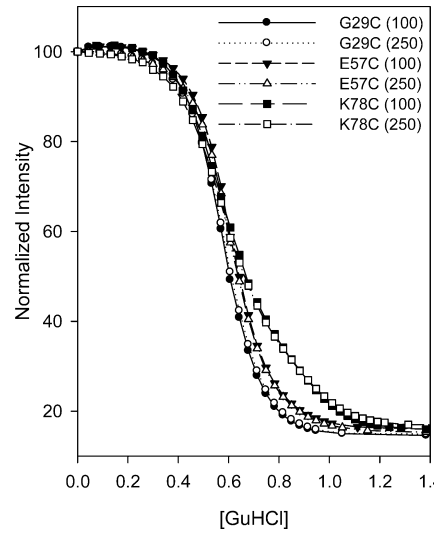

FIGURE 1: Normalized fluorescence intensity as a function of guanidine hydrochloride concentration for the dimers of the G29C, E57C, and K78C mutants cross-linked using bismaleimide 2 from Figure 2. Titrations were conducted at starting sodium chloride concentrations of 100 and 250 nM.

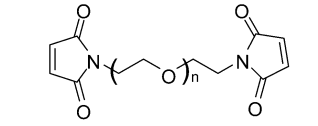

1. n = 0
2. n = 1
3. n = 2
4. n = 3

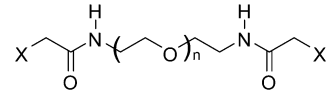

5. X = Br, n = 0
6. X = Br, n = 1
7. X = Br, n = 2
8. X = Br, n = 3
9. X = I, n = 0
10. X = I, n = 1
11. X = I, n = 2
12. X = I, n = 3

FIGURE 2: Cross-linkers used in this study included bismaleimides **1**−**4**, bromoacetamides **5**−**8**, and iodoacetamides **9**−**12**.

same proteins after treatment with the monovalent controls HEM and BHA.

The average change in free energy for the control (HEM) modified monomers relative to unmodified protein ($\Delta G_{cysteine\ standard} - \Delta G_{HEM\ monomer}$) is only 0.1 ± 0.1 kcal/mol, in other words, unchanged within experimental error. While approximately 25% of the HEM-treated proteins are unmodified, on the basis of Ellman's assay, this small change in stability still seems to indicate that derivatization of cysteine with maleimide does not by itself cause significant stability changes. The stability changes for the wild type are somewhat greater, perhaps since the absence of cysteines means reactions with other side chains, with more deleterious effects, are more likely.

In line with this idea, when enough monomer could be recovered for stability measurements after treatment with bismaleimide, rather larger changes in stability are found (data not shown). The average change in free energy for the bismaleimide-treated monomers is 1.2 ± 0.1 kcal/mol. This likely reflects the fact that while reaction with cysteine is

Table 1: Stability Parameters from Guanidine Hydrochloride Denaturation of Unmodified Cysteine Mutants and Controls

	untreated monomers[a]			HEM-treated monomers[b]			BHA-treated monomers[b]		
protein	ΔG_{H_2O}[c]	C_m[d]	m_{GuHCl}[e]	ΔG_{H_2O}[c]	C_m[d]	m_{GuHCl}[e]	ΔG_{H_2O}[c]	C_m[d]	m_{GuHCl}[e]
G29C	4.4	0.60	7.24	4.3	0.61	7.02	4.4	0.62	7.14
G50C	4.7	0.71	6.58	4.6	0.73	6.34	4.8	0.73	6.49
E57C	4.8	0.73	6.54	4.6	0.75	6.20	4.7	0.75	6.24
A60C	4.5	0.66	6.76	4.4	0.67	6.50	4.3	0.67	6.42
K70C	4.8	0.74	6.47	4.9	0.76	6.47	4.5	0.74	6.11
K78C	5.2	0.80	6.42	5.0	0.81	6.20	4.9	0.81	6.05
R105C	2.9	0.46	6.22	2.8	0.47	5.95	2.9	0.47	6.17
A112C	4.7	0.71	6.61	4.8	0.73	6.49	4.8	0.74	6.48
K134C	4.7	0.70	6.73	4.7	0.72	6.49	4.4	0.67	6.50
wild type	5.4	0.82	6.56	5.1	0.83	6.11	5.2	0.84	6.24

[a] In 100 mM sodium chloride, 25 mM sodium phosphate (pH 7.0), and 0.5 mM TCEP at 20 °C. The wild type was titrated under identical conditions except for the absence of TCEP. [b] In 250 mM sodium chloride, 25 mM sodium phosphate (pH 7.0), and 0.5 mM TCEP at 20 °C. The wild type was titrated under identical conditions except for the absence of TCEP. [c] Free energy difference between native and denatured states in the absence of denaturant in units of kilocalories per mole. The error was estimated to be ±0.1 kcal/mol. [d] Midpoint concentration (concentration of guanidine hydrochloride at which half of the protein molecules are denatured) in units of molar. The error was estimated to be ±0.01 M. [e] Slope value (change in free energy with respect to the change in guanidine hydrochloride concentration) in units of kilocalories per mole per molar. The error was estimated to be ±0.1 kcal mol^{-1} M^{-1}.

preferred, it is not the only possible course of reaction. Many of these monomers have probably been intramolecularly cross-linked.

Many of the cross-linked dimers exhibit clear biphasic unfolding behavior, as most clearly shown in Figure 1 for the dimer of K78C. Therefore, the three-state model describing the thermodynamics of unfolding for these dimers as outlined in Materials and Methods was fit to data for these proteins. Our model assumes at any given guanidine hydrochloride concentration only three species are significantly populated. Those species are described as follows: cross-linked dimer with both monomer units folded (N−N), cross-linked dimer with one monomer unit folded and one unfolded (N−D), and cross-linked dimer with both monomer units unfolded (D−D). Also, we assume that each phase of the denaturation can be described by a single cooperative transition, and in fitting, we assume that one-half of the fluorescence difference between the N−N state and the D−D state is lost in the N−D state. Each phase can be characterized by a unique slope value and free energy. These values are given in Table 2 for dimers attached with the bismaleimide cross-linker family and in Table 3 for selected dimers resulting from cross-linking with the bishaloacetamide family. The results of three-state fits to the denaturations of the bismaleimide dimers at 100 mM NaCl are available as Supporting Information. Other models of unfolding are theoretically possible; for example, both monomers might simultaneously partially unfold and then later completely unfold cooperatively (N−N to I−I to D−D). This cannot be completely ruled out, but it seems unlikely because it is widely thought that the first structure to unfold in nuclease is the C-terminal helix containing the tryptophan and postulating a partially unfolded intermediate that retains tryptophan fluorescence would be without precedent.

In particular for long linkers, the transitions of some proteins no longer exhibit clear three-state behavior. All of the data were also analyzed with a two-state model, and those results are given in Table 4 for dimers attached with the bismaleimide cross-linked dimers and in Table 5 for selected dimers resulting from cross-linking with the bishaloacetamide family. The results of two-state fits to the denaturations of the bismaleimide dimers at 100 mM NaCl are available as Supporting Information. The fit of the data to the linear two-state model is given as well to aid in evaluation of the reliability of this model. Normally, for monomeric mutants, we consider a value of R^2 of <0.999 an indication of poor-quality data.

Lastly, a description of the error associated with the nonlinear regressions to the three-state model is needed. The average errors returned by the fitting program for ΔG_{H_2O} were ±0.2 kcal/mol for the first (N−N ⇌ N−D) transition and ±0.5 kcal/mol for the second (N−D ⇌ D−D) transition. For both transitions, the errors in m_{GuHCl} were close to ±0.5 kcal mol^{-1} M^{-1}. However, these average numbers hide a large range. The lowest reported uncertainties for m_{GuHCl} were ±0.07 kcal mol^{-1} M^{-1} and the highest ±1.8 kcal mol^{-1} M^{-1}. The lowest reported uncertainties for ΔG_{H_2O} were ±0.03 kcal/mol and the highest ±1.8 kcal/mol. Uncertainty in one parameter was well-correlated with uncertainty in others. Specifically, when uncertainty in the parameters for the slope was high, so was the uncertainty in stability. Uncertainty in the first transition also correlated extremely well with uncertainty in the parameters for the second transition.

The error reported by the fitting program was generally lowest when there were two distinct transitions, i.e., when a three-state unfolding was clearly present and the data constrained the possible range of solutions. Errors were higher when there were not two distinct transitions visible. In this case, the available data undetermined the fitting of the complex equation for the three-state model and a fairly wide range of possible solutions exist. Nevertheless, it should be noted that similar parameters for the two transitions were still returned when fitting these cases, despite their higher uncertainty. The major exception to this trend was R105C, which has two transitions but had high uncertainties. This is presumably due to the fact that it is partially unfolded even in the absence of denaturant and no native baseline exists to constrain the fits. The values for m_{GuHCl} in the first transition, especially for the shortest linkers, are suspiciously high, and it seems likely that the relatively large error returned by the fitting program for the various R105C dimers is, if anything, too low. In summary, except for R105C, when there are large differences between m_{GuHCl} and ΔG_{H_2O} for the two transitions in Table 2 or 3, the confidence in these values is high. When

Table 2: Denaturation Parameters Obtained by Nonlinear Regression of Maleimide-Cross-Linked Dimers to a Three-State Model (250 mM NaCl titrations)

protein	cross-linker	$\Delta G^1_{H_2O}$[a]	C^1_m[b]	m^1_{GuHCl}[c]	$\Delta G^2_{H_2O}$[a]	C^2_m[b]	m^2_{GuHCl}[c]
G29C	$n = 0$	3.6	0.56	6.4	3.8	0.62	6.2
	$n = 1$	3.5	0.56	6.2	3.9	0.61	6.4
	$n = 2$	3.7	0.57	6.5	3.7	0.60	6.2
	$n = 3$	3.8	0.55	6.9	4.2	0.63	6.7
G50C	$n = 0$	2.5	0.77	3.2	4.0	0.68	5.8
	$n = 1$	2.2	0.84	2.6	3.9	0.66	5.9
	$n = 2$	3.4	0.73	4.7	3.8	0.71	5.4
	$n = 3$	3.7	0.69	5.4	3.8	0.71	5.4
E57C	$n = 0$	3.3	0.64	5.2	2.8	0.60	4.7
	$n = 1$	3.5	0.63	5.6	2.8	0.58	4.8
	$n = 2$	3.3	0.65	5.1	3.3	0.59	5.6
	$n = 3$	3.5	0.64	5.5	3.2	0.61	5.2
A60C	$n = 0$	2.5	0.58	4.3	3.6	0.56	6.5
	$n = 1$	2.4	0.57	4.2	3.7	0.54	6.8
	$n = 2$	3.0	0.59	5.1	3.4	0.56	6.0
	$n = 3$	3.1	0.59	5.3	3.2	0.55	5.8
K70C	$n = 0$	2.6	0.64	4.0	4.5	0.69	6.5
	$n = 1$	3.5	0.71	4.9	3.1	0.60	5.2
	$n = 2$	3.3	0.64	5.2	4.2	0.66	6.3
	$n = 3$	3.8	0.67	5.7	3.8	0.68	5.6
K78C	$n = 0$	3.4	0.53	6.5	2.4	0.79	3.0
	$n = 1$	3.5	0.52	6.7	3.0	0.73	4.1
	$n = 2$	3.2	0.62	5.2	2.4	0.76	3.2
	$n = 3$	3.5	0.63	5.5	4.7	0.80	5.9
R105C	$n = 0$	1.2	0.11	11.2	0.5	0.11	4.4
	$n = 1$	1.1	0.14	7.9	0.3	0.06	4.7
	$n = 2$	1.5	0.16	9.2	0.6	0.19	3.1
	$n = 3$	1.6	0.19	8.3	0.6	0.17	3.6
A112C	$n = 0$	2.4	0.48	5.0	2.0	0.63	3.2
	$n = 1$	3.2	0.57	5.7	2.2	0.61	3.6
	$n = 2$	3.9	0.64	6.1	3.7	0.69	5.3
	$n = 3$	3.6	0.78	4.6	4.3	0.70	6.1
K134C	$n = 0$	2.6	0.55	4.7	3.9	0.70	5.6
	$n = 1$	3.5	0.63	5.5	4.3	0.73	5.9
	$n = 2$	3.7	0.64	5.7	4.1	0.72	5.7
	$n = 3$	3.3	0.67	4.9	3.7	0.70	5.3

[a] Stability of protein to reversible denaturation in units of kilocalories per mole fit by nonlinear regression to a three-state unfolding model. A superscript 1 indicates the value is for the first (N−N ⇌ N−D) transition, and a superscript 2 indicates it is for the second (N−D ⇌ D−D) transition. The average error, as returned by the fitting program, was ±0.2 kcal/mol in the former and ±0.5 kcal/mol in the latter. [b] Midpoint concentration (concentration of guanidine hydrochloride at which half of the protein molecules are denatured) in units of molar calculated from the values of ΔG_{H_2O} and m_{GuHCl} returned by nonlinear regression to a three-state model. A superscript indicates whether the value is for the first (N−N ⇌ N−D) or second (N−D ⇌ D−D) transition. [c] Slope value (change in free energy with respect to change in guanidine hydrochloride concentration) fit by nonlinear regression to a three-state unfolding model. A superscript indicates whether the value is for the first (N−N ⇌ N−D) or second (N−D ⇌ D−D) transition. The average error, as returned by the fitting program, was ±0.6 kcal mol^{-1} M^{-1} in the former and ±0.5 kcal mol^{-1} M^{-1} in the latter.

differences are relatively small, uncertainties are high and the actual difference might possibly be larger, or completely negligible.

Thermal Denaturations. The thermal unfolding of the cross-linked dimers was followed by fluorescence spectroscopy, except for the dimers of the R105C mutant, which is too unstable to produce reliable native baseline data needed for the data analysis. As previously found for the BMH-cross-linked dimers, even in 100 mM NaCl, the data were well fit in all cases by a standard two-state model. The results of this analysis are listed in Tables 6, where T_m is that temperature at which half of the protein molecules are unfolded and ΔH_{vH} is the van't Hoff enthalpy of unfolding at the transition temperature.

Table 3: Parameters Obtained by Nonlinear Regression of GuHCl Denaturation of Haloacetamide-Cross-Linked Dimers in 250 mM NaCl and 25 mM sodium phosphate (pH 7.0) to a Three-State Model

protein	cross-linker	$\Delta G^1_{H_2O}$[a]	C^1_m[b]	m^1_{GuHCl}[c]	$\Delta G^2_{H_2O}$[a]	C^2_m[b]	m^2_{GuHCl}[c]
G29C	Br, $n = 0$	3.3	0.59	5.6	3.4	0.58	5.8
	Br, $n = 1$	3.4	0.55	6.2	3.6	0.60	6.0
	Br, $n = 2$	3.5	0.55	6.4	4.0	0.62	6.5
	I, $n = 0$	3.3	0.58	5.7	3.5	0.58	6.0
	I, $n = 1$	3.5	0.57	6.1	3.6	0.59	6.1
	I, $n = 2$	3.2	0.58	5.5	3.4	0.58	5.9
G50C	Br, $n = 0$	3.3	0.80	4.1	3.8	0.70	5.4
E57C	Br, $n = 0$	3.4	0.60	5.7	6.0	0.71	8.4
	Br, $n = 1$	2.8	0.65	4.3	3.5	0.60	5.8
	Br, $n = 2$	3.0	0.65	4.6	3.8	0.62	6.1
	I, $n = 0$	3.3	0.59	5.6	5.3	0.70	7.6
	I, $n = 1$	2.9	0.65	4.5	3.5	0.61	5.8
	I, $n = 2$	2.8	0.67	4.2	4.0	0.62	6.5
A60C	Br, $n = 0$	3.4	0.62	5.5	2.9	0.57	5.1
K70C	Br, $n = 0$	3.8	0.78	4.9	2.5	0.61	4.1
K78C	Br, $n = 0$	3.6	0.66	5.5	2.4	0.61	4.0
	Br, $n = 1$	4.0	0.67	5.9	1.8	0.59	3.1
	Br, $n = 2$	3.9	0.63	6.2	6.4	0.86	7.4
	I, $n = 0$	3.5	0.64	5.5	2.2	0.69	3.2
	I, $n = 1$	3.3	0.66	5.0	3.2	0.60	5.3
	I, $n = 2$	3.9	0.62	6.3	5.3	0.88	6.0
R105C	Br, $n = 0$	1.1	0.15	7.4	1.2	0.37	3.2
A112C	Br, $n = 0$	3.7	0.55	6.7	4.9	0.94	5.2
K134C	Br, $n = 0$	3.6	0.95	3.8	1.5	0.43	3.5

[a] Stability of protein to reversible denaturation in units of kilocalories per mole fit by nonlinear regression to a three-state unfolding model. A superscript indicates whether the value is for the first (N−N ⇌ N−D) or second (N−D ⇌ D−D) transition. The average error, as returned by the fitting program, was ±0.2 kcal/mol in the former and 0.5 kcal/mol in the latter. [b] Midpoint concentration (concentration of guanidine hydrochloride at which half of the protein molecules are denatured) in units of molar calculated from the values of ΔG_{H_2O} and m_{GuHCl} returned by nonlinear regression to a three-state unfolding model. A superscript indicates whether the value is for the first (N−N ⇌ N−D) or second (N−D ⇌ D−D) transition. [c] Slope value (change in free energy with respect to the change in guanidine hydrochloride concentration) fit by nonlinear regression to a three-state unfolding model. A superscript indicates whether the value is for the first (N−N ⇌ N−D) or second (N−D ⇌ D−D) transition. The average error, as returned by the fitting program, was ±0.5 kcal mol^{-1} M^{-1} for both transitions.

DISCUSSION

Protein-denatured states have been reviewed several times recently (*27–30*). Arguably, the denatured state of staphylococcal nuclease (nuclease) has been more intensively studied and is better understood than that of any other protein. Unfortunately, the results of the study of nuclease are in many ways contradictory and confusing and thus illustrate how much remains to be learned about denatured states.

Still, we know that nuclease has, as do virtually all proteins examined, significant amounts of residual structure in the denatured state. The "structure" of denatured nuclease has been determined by NMR techniques by Shortle's group (*31–34*). They demonstrated that nuclease retains long-range structure similar to that of the native state even under the highly denaturing conditions of 8 M urea. However, we know little about the relative flexibility of the different parts of the molecule. A particular question of interest is how far out the energetic "sphere of influence" of a denatured protein extends. In other words, how much space is required for the denatured protein to behave as if it is, in effect, isolated from other protein molecules?

As described in the Supporting Information, we synthesized series of homobifunctional cross-linkers with differing lengths, based on a polyethylene glycol linker. These cross-

Table 4: Values from a Fit of Guanidine Hydrochloride Denaturation of Bismaleimide-Cross-Linked Dimers in 250 mM NaCl to a Two-State Model

protein	cross-linker	ΔG_{H_2O}	C_m	m_{GuHCl}	R^2
G29C	$n = 0$	4.3	0.59	7.30	0.999
	$n = 1$	4.3	0.58	7.26	0.999
	$n = 2$	4.4	0.59	7.51	0.999
	$n = 3$	4.4	0.59	7.41	0.999
G50C	$n = 0$	4.4	0.70	6.22	0.994
	$n = 1$	4.3	0.71	6.07	0.994
	$n = 2$	4.7	0.71	6.63	0.999
	$n = 3$	4.7	0.70	6.63	0.999
E57C	$n = 0$	4.0	0.62	6.56	0.998
	$n = 1$	4.2	0.61	6.83	0.998
	$n = 2$	4.4	0.62	7.20	0.999
	$n = 3$	4.5	0.63	7.18	0.999
A60C	$n = 0$	4.0	0.57	7.11	0.997
	$n = 1$	4.0	0.55	7.15	0.995
	$n = 2$	4.2	0.57	7.43	0.998
	$n = 3$	4.2	0.57	7.42	0.999
K70C	$n = 0$	4.0	0.66	6.08	0.993
	$n = 1$	4.9	0.65	7.45	0.999
	$n = 2$	4.5	0.65	6.95	0.999
	$n = 3$	4.9	0.67	7.35	0.999
K78C	$n = 0$	2.4	0.66	3.69	0.968
	$n = 1$	2.9	0.64	4.50	0.987
	$n = 2$	3.3	0.68	4.80	0.998
	$n = 3$	3.5	0.75	4.69	0.998
R105C	$n = 0$	1.1	0.14	7.88	0.941
	$n = 1$	1.3	0.14	9.20	0.979
	$n = 2$	1.1	0.21	5.46	0.919
	$n = 3$	1.6	0.22	7.10	0.952
A112C	$n = 0$	2.4	0.57	4.20	0.990
	$n = 1$	3.1	0.60	5.24	0.989
	$n = 2$	4.4	0.67	6.59	0.998
	$n = 3$	5.7	0.74	7.65	0.999
K134C	$n = 0$	3.2	0.63	5.08	0.999
	$n = 1$	4.2	0.68	6.26	0.999
	$n = 2$	4.4	0.69	6.34	0.999
	$n = 3$	4.4	0.69	6.31	0.999

Table 5: Values from a Fit of Guanidine Hydrochloride Denaturation of Bishaloacetamide-Cross-Linked Dimers in 250 mM NaCl to a Two-State Model

protein	cross-linker	ΔG_{H_2O}	C_m	m_{GuHCl}	R^2
G29C	Br, $n = 0$	4.2	0.58	7.26	0.999
	Br, $n = 1$	4.1	0.58	7.11	0.999
	Br, $n = 2$	4.3	0.59	7.36	0.999
	I, $n = 0$	4.3	0.58	7.39	0.999
	I, $n = 1$	4.3	0.59	7.38	0.999
	I, $n = 2$	4.2	0.58	7.29	0.999
G50C	Br, $n = 0$	5.0	0.74	6.78	0.999
E57C	Br, $n = 0$	4.6	0.65	6.96	0.993
	Br, $n = 1$	4.2	0.62	6.80	0.997
	Br, $n = 2$	4.5	0.63	7.07	0.997
	I, $n = 0$	4.4	0.65	6.84	0.996
	I, $n = 1$	4.2	0.62	6.89	0.998
	I, $n = 2$	4.6	0.63	7.26	0.997
A60C	Br, $n = 0$	4.3	0.60	7.17	0.998
K70C	Br, $n = 0$	4.9	0.71	6.93	0.999
K78C	Br, $n = 0$	4.1	0.65	6.40	0.997
	Br, $n = 1$	3.8	0.66	5.76	0.993
	Br, $n = 2$	3.9	0.74	5.21	0.997
	I, $n = 0$	3.3	0.67	4.83	0.989
	I, $n = 1$	4.5	0.63	7.14	0.999
	I, $n = 2$	3.4	0.74	4.57	0.998
R105C	Br, $n = 0$	1.2	0.28	4.22	0.940
A112C	Br, $n = 0$	2.6	0.74	3.46	0.988
K134C	Br, $n = 0$	4.6	0.70	6.51	0.999

linkers are shown in Figure 2. The sulfur−sulfur separations expected for each cross-linker at maximal extension are listed in Table 7. Three different thiol specific functional groups were used: maleimide, bromoacetamide, and iodoacetamide. Previous work with a single length of cross-linker (*22*) established the specificity and completeness of modification with the maleimide cross-linker and that the impact of alkylation itself upon protein stability was not extraordinary. Results presented in the Supporting Information, including those with a new control which is more polar than our previous control, reaffirm that earlier conclusion. The changes in protein denaturation behavior observed are therefore due to the constrained presence of another protein molecule, not to some other effect of the modification.

The alkylation of cysteine with bromoacetamide and iodoacetamide results in identical products, but the two groups differ in their specificity of reaction with thiol. The haloacetamides result in an adduct quite different from the maleimide. All proteins were reacted with the complete range of bismaleimide cross-linkers. A selection of proteins reacted with bishaloacetamide cross-linkers were also examined. These serve as yet another set of controls, confirming that similar behavior is found with cross-linkers similar in length, despite differences in the precise chemical group used to covalently link the proteins.

One effect that was observed, particularly prominently for short cross-linker lengths, was a tendency for the native baseline to rise with the addition of guanidine hydrochloride. It seemed likely that this effect was due to electrostatic interactions between the linked native states that are masked as the addition of guanidine hydrochloride increases the ionic strength. Running the titrations in a buffer containing 250 mM NaCl rather than our normal 100 mM NaCl resulted in flatter baselines. A further advantage is that attenuating charge−charge interactions in both the native and denatured states should emphasize the influence of steric effects in the denatured state, something of particular interest. While this discussion will focus on the data obtained for dimers and the controls at 250 mM NaCl, the results at lower ionic strengths are available as Supporting Information.

It should be noted that such an increase in sodium chloride concentration has no significant effect upon the denaturation behavior of the (monomeric) wild type. We will return to this point later; however, briefly, several dimers show distinct shifts in the midpoint of denaturation to lower concentrations of guanidine hydrochloride with higher concentrations of sodium chloride, while others show virtually no change other than a flatter native baseline.

Solvent Denaturation of Cross-Linked Dimers. As expected, the guanidine hydrochloride denaturations of the unmodified standards and the HEM-modified monomers fit the two-state model of denaturation well, unfolding cooperatively in one transition. As inspection of Figure 1 shows, this is not true for many of the maleimide-cross-linked dimers. In particular, K78C and R105C show obvious deviations from the sigmoid behavior of the two-state model. Although more subtle when looking at the raw denaturation curves, K70C, A112C, and K134C for some linker lengths do not have the strictly linear relationship between guanidine hydrochloride concentration and free energy predicted by the two-state model (data not shown). On the other hand, many of the dimers, especially those with longer linkers, do seem to have two-state denaturation curves.

This qualitative assessment is conveyed in a slightly more quantitative manner by comparing the protein stabilities determined by fitting to the two-state model for the HEM-

Table 6: Thermal Denaturation Parameters of Cysteine Mutants, HEM-Alkylated Monomeric Controls, and Bismaleimide-Cross-Linked Dimers

	untreated standard		HEM (control)		dimer, $n = 0$		dimer, $n = 1$		dimer, $n = 2$		dimer, $n = 3$	
protein	T_m[a]	ΔH_{vH}[b]	T_m[a]	ΔH_{vH}[b]	T_m[a]	ΔH_{vH}[b]	T_m[a]	ΔH_{vH}[b]	T_m[a]	ΔH_{vH}[b]	T_m[a]	ΔH_{vH}[b]
G29C	48.4	81	45.9	90	44.3	93	44.9	95	44.0	99	44.5	92
G50C	50.4	77	49.3	90	47.9	103	48.7	108	48.3	100	47.9	101
E57C	52.1	77	51.2	85	48.0	96	48.2	93	47.8	94	48.0	95
A60C	49.4	74	48.8	86	46.5	101	46.5	104	45.8	98	45.5	93
K70C	50.2	75	48.4	67	43.4	105	43.4	94	43.5	108	44.3	89
K78C	53.4	83	47.6	51	45.5	77	45.0	68	45.3	61	47.1	53
R105C	41.9	58	ND[c]	ND[c]	ND[c]	ND[c]	ND[c]	ND[c]	ND[c]	ND[c]	ND[c]	ND[c]
A112C	50.2	77	48.4	75	45.3	111	46.3	103	47.0	88	47.9	73
K134C	50.1	77	49.1	80	46.3	94	46.6	91	46.3	93	46.4	81
wild type	53.0	86	ND[c]	ND[c]	ND[c]	ND[c]	ND[c]	ND[c]	ND[c]	ND[c]	ND[c]	ND[c]

[a] Melting temperature (temperature at which half of the protein molecules are unfolded) using fluorescence as probe of structure in units of degrees Celsius. The error was estimated to be ±0.3 °C. [b] van't Hoff enthalpy (enthalpy of denaturation estimated from the van't Hoff equation) using fluorescence as probe of structure in units of kilocalories per mole. The error was estimated to be ±2 kcal/mol. [c] Not determined.

Table 7: Maximal Sulfur−Sulfur Distances As Determined by Molecular Modeling

cross-linker	S−S distance (Å)[a]
1, $n = 0$	10.5
2, $n = 1$	14.6
3, $n = 2$	17.3
4, $n = 3$	21.3
6 and **9**, $n = 0$	11.9
7 and **10**, $n = 1$	13.8
8 and **11**, $n = 2$	16.4

[a] The maximal sulfur−sulfur distance was calculated with Hyperchem 7 Molecular Modeling (Hypercube Inc.) after each cross-linker was optimized in an extended conformation with all possible regio- and stereochemistries for sulfur addition considered.

alkylated controls and the dimers made using the various length cross-linkers. These differences, listed in Table 8, are striking. For some proteins, for example, G29C in Figure 1, there is never any experimentally significant difference between the monomeric control and the dimeric protein, regardless of linker length. For other proteins, for example, K78C, the dimeric protein is always significantly different from the monomeric control. For other proteins, for example, K70C, there are small differences at the shortest linker lengths that become experimentally insignificant as lengths increase.

It is important to recognize that a large apparent stability difference is not a valid measure of change in stability. Rather, what it does indicate is a case in which the two-state model has failed. Where the fit to the two-state model is good for the dimer, there is little or no significant stability difference between the dimer and monomeric control. Where the fit is poor, which in most cases corresponds to those protein dimers in which there is clear-cut biphasic unfolding, there is an apparent energy difference.

This biphasic unfolding behavior observed for some bismaleimide-cross-linked dimers can be accounted for by postulating a three-state thermodynamic model for the denaturation. These three states are a cross-linked dimer with both monomer subunits folded (N−N), a cross-linked dimer with one monomer subunit folded and one unfolded (N−D), and a cross-linked dimer with both monomer subunits unfolded (D−D). We assume that each of the monomer subunits in the maleimide-cross-linked dimers are independent folding units. The first transition follows the unfolding of one of the monomer subunits, while the second transition follows the unfolding of the second monomer subunit. It is expected that these transitions are different. The first subunit unfolds while it is covalently bonded to another folded subunit, and the second subunit unfolds while it is bonded to an unfolded subunit. These are distinctly different denaturations, and hence, each should be characterized by a unique free energy and slope value. The derivation of our three-state unfolding mathematical model has been described previously (*22*). When nonlinear regression is used to fit the data to the three-state model, distinctly different m_{GuHCl} and ΔG_{H_2O} values are often found for the two transitions (Tables 2 and 3). Each of these transitions differs to a lesser or greater extent from those found for the modified monomers we use as controls (Table 1).

Comparison of Table 2 to Table 4 and of Table 3 to Table 5 shows that if the two-state fit is good for the dimer then the three-state fit generally, although not always, yields values for the component transitions that are very similar to one another and to the values from the two-state fit. That there is disagreement between the three sets of values is not unexpected given the relative complexity of the three-state model and the lack of two clearly resolved transitions in the data which the two-state model fits. In other words, in many cases there is no significant difference between the results of the three-state fit and the two-state fit. There are obvious variations with the linker length and position of cross-linker attachment to which we shall return.

More interesting are those dimers for which there are two distinct transitions. This would include K78C, R105C, and A112C dimers with all linker lengths and K70C, K134C, and, to a lesser extent, E57C dimers with shorter linkers. Here the differences between the two transitions returned by fitting to the three-state model are much more meaningful. Some trends are found among cases where the three-state model is clearly more appropriate. Previously, when we examined the effect of only a single linker length (*22*), it appeared that the stability, $\Delta G^2_{H_2O}$, of the transition between the N−D and D−D states was usually smaller than the stability determined for the first transition ($\Delta G^1_{H_2O}$), that between the N−N and N−D states. That generalization is still true, but now we find more exceptions, especially for long linkers.

We see that there is more variation in the values of stability, slope, and midpoint for the second transition as a function of linker length than for the first transition. While this variation does not seem to be a simple linear progression with an increase in linker length, there is an overall tendency

Table 8: Apparent Differences in Protein Stability between the Monomeric HEM-Alkylated Proteins and the Cross-Linked Dimers [$\Delta\Delta G_{H_2O} = \Delta G_{H_2O}(HEM) - \Delta G_{H_2O}(dimer)$][a]

	250 mM NaCl				100 mM NaCl			
protein	$n = 0$	$n = 1$	$n = 2$	$n = 3$	$n = 0$	$n = 1$	$n = 2$	$n = 3$
G29C	0.0	0.0	−0.1	−0.1	0.0	0.0	−0.1	−0.2
G50C	0.2	0.3	−0.1	−0.1	−0.3	−0.2	−0.1	0.0
E57C	0.6	0.4	0.2	0.1	0.3	0.3	−0.1	−0.2
A60C	0.4	0.4	0.2	0.2	0.3	0.0	0.0	0.1
K70C	0.9	0.0	0.4	0.0	0.6	0.0	0.1	−0.1
K78C	2.6	2.1	1.7	1.5	2.5	2.0	1.6	1.4
R105C	1.7	1.5	1.7	1.2	1.6	1.3	1.6	1.3
A112C	2.4	1.7	0.4	−0.9	2.4	1.5	0.0	−1.0
K134C	1.5	0.5	0.3	0.3	1.2	0.0	0.0	0.2

[a] These apparent stabilities are as determined by a fit to a two-state model.

for the values of the first and second transitions to converge with an increase in length. In other words, the denaturation begins to look like a two-state transition.

Previously (*22*), we had drawn the conclusion that the similarity of the first transition to that of monomeric controls and the generally reduced slope values for the second transition pointed to interactions between the denatured states as the cause of altered behavior for the second transition. Although it does not prove that changes in the denatured state are at the heart of this three-state behavior, this tendency for the two transitions to converge with an increasing linker length is consistent with that interpretation.

Thermal Denaturation of Cross-Linked Dimers. Thermal denaturations of the bismaleimide-cross-linked dimers, HEM-modified monomers, and unmodified cysteine standards were performed using fluorescence as a probe of structure. The temperature required to half-unfold the protein (midpoint temperature, T_m) and the van't Hoff enthalpy (ΔH_{vH}) of unfolding at the T_m were obtained from the analysis of thermal denaturation data.

These results are listed in Table 6. T_m is down slightly for all the bismaleimide dimers relative to those of HEM-modified monomers, but virtually invariant as a function of linker length. The van't Hoff enthalpies for eight of the bismaleimide-cross-linked dimers are significantly higher than those of the untreated cysteine standards. The T_m is, within experimental error, virtually invariant as cross-linker length varies for a given mutant. However, the van't Hoff enthalpy tends to drop slightly. As observed previously, the thermal unfolding data of the dimers do not reveal three-state thermodynamic behavior but do generally show elevated van't Hoff enthalpies for the dimers relative to those of the HEM-modified monomers. However, the dimers which fit the two-state solvent denaturation model well, for example, G29C, have van't Hoff enthalpies very similar to those of the HEM-modified monomers. The more pronounced the three-state behavior in solvent denaturation, the greater the elevation of ΔH_{vH} in thermal denaturation. Yet, even in these cases, the value of ΔH_{vH} tends to drop toward the value found in the HEM-modified monomer as the linker length increases. Thus, there is obvious and consistent agreement between the thermal and chemical denaturation behavior for different sites of cross-linking and for different cross-linker lengths.

Positional Variation. There is clear variation in behavior with the position of alkylation. The sites chosen for derivatization are all solvent-exposed in the wild type but are scattered about the surface to provide a global sampling of behavior. Some positions have virtually no difference in either solvent or thermal denaturation behavior between alkylated monomeric control and the dimers. The most clear-cut case of this sort is G29C. G50C, E57C, and A60C show less clear-cut two-state behavior for the shorter linkers, but denaturation of the dimers is generally fairly similar to that of the monomers. K70C and K134C clearly are three-state for the shortest linkers but are two-state as the linker becomes longer. A112C has a three-state solvent denaturation for all lengths, although the thermal denaturation of the longest linker seems to be fairly similar to that of the monomer. K78C and R105C are unambiguously different from the corresponding monomeric controls for all linker lengths in both solvent and thermal denaturation.

When these positions are plotted on the protein structure, a clear pattern is obvious. The positions with the most pronounced three-state behavior, K78C, R105C, and A112C, although well separated in primary structure, are all close to the C-terminal helix of nuclease (Figure 3). K70C is more distant, but not as far as G29C, G50C, E57C, and A60C. K134C is at the very end of the C-terminal helix.

There are several indications that the C-terminus of nuclease is among the first parts of the protein to lose all structure. Most notable is the more rapid loss of fluorescence from tryptophan 140 than for a tryptophan added into the major hydrophobic core in the V66W mutant (*35–38*). This helix may or may not be a separate domain; however, there is no question that it is not an integral part of the β-barrel which makes up the largest part of the protein and may unfold first (*39–41*). It is plausible that it is more disordered and enjoys greater conformational freedom in the denatured state than the rest of the protein, which is known to, overall, retain an expanded nativelike structure (*31, 33*).

Conformational Entropy and Protein Stability. The principal force of destabilizing the structure of protein is believed to be the high conformational entropy of the denatured state. Obviously, the flexible denatured state has much greater conformational freedom than the native state of a protein. It has been convincingly argued that this conformational freedom and, thus, the entropy of the protein's denatured state are limited by the volume occupied by the protein itself (*42*). It is expected that minimizing the conformational degrees of freedom in the denatured state would lead to destabilization of the denatured state and hence stabilization of the native state. However, the volume effect also can be a possible reason for increases in stabilities sometimes observed when proteins are linked to solid supports (*43–46*).

The denatured state of a protein is not a single discrete, well-defined conformation but an ensemble of conformations.

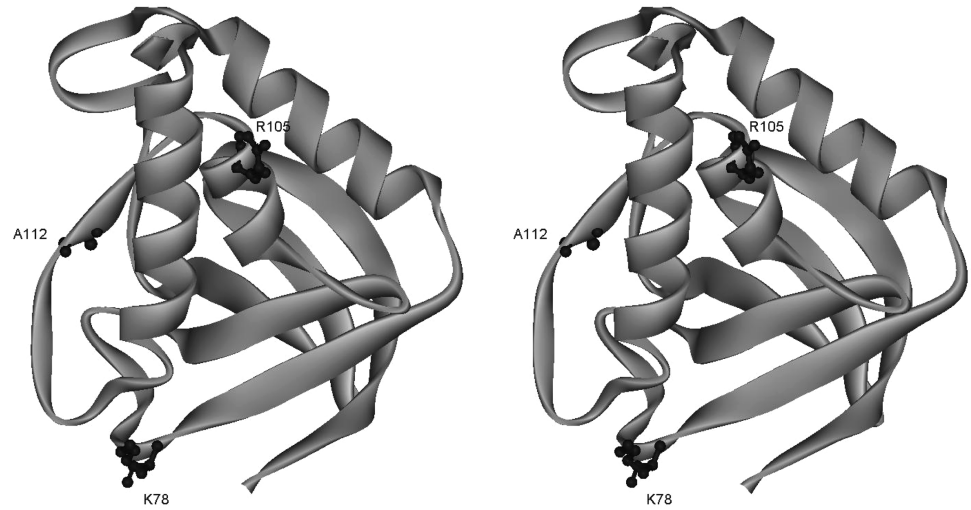

FIGURE 3: Stereo ribbon diagram of staphylococcal nuclease (Protein Data Bank entry 1EY0) with the main and side chains of K78, R105, and A112 shown as balls and sticks. The C-terminal helix bisects the middle of the protein in this viewing angle, with the C-terminus itself at the top of the figure.

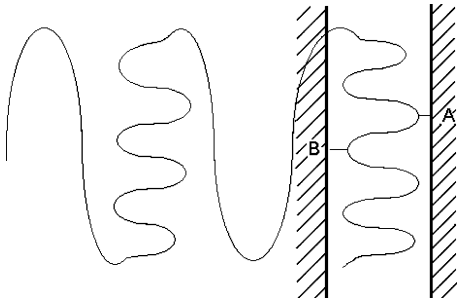

FIGURE 4: Representation of a hypothetical denatured state conformation. Linkage at point A is possible in this conformation, but linkage at point B is not because this would require the adjacent object and the denatured protein to occupy the same space.

Consider for a moment the possibilities of restraining the conformational freedom of the denatured protein by cross-linking a protein to some object, which could be a macroscopic surface or another protein, either native or denatured. In Figure 4, a particular hypothetical denatured state conformation linked to such an object is illustrated schematically. In this conformation, suppose that attachment point A is on the surface or near it. A linker of modest length allows attachment to another object. However, another potential attachment point, B, is not near the surface of this conformation of the denatured state. Attachment at point B to another object with a short linker is not possible. Of course, the conformationally flexible denatured state can adopt another conformation, but the conformation illustrated in the figure and any others which significantly sequester the attachment from ready access are barred to it. In other words, the conformational freedom of the denatured state, the principal property favoring it relative to the native state, is reduced.

Again, the attachment points chosen are all solvent-exposed in the native state, but since the residual structure in the denatured state is known to be nativelike, it seems plausible that these sites are usually solvent exposed in the denatured state. Given the minimal impact for the effect of cross-linking at, for example, G29C, it seems that this position is never inaccessible, even with our shortest cross-linker. On the other hand, even though they are solvent-exposed, it is easy to imagine looking at Figure 3 that another protein tethered at any of these points could significantly restrict the conformational freedom of the C-terminus if the helix detaches from the remainder of the structure, as we hypothesize that it does.

In short, the data presented here indicate clearly that excluded volume effects are real and readily observable. However, they also indicate that for most regions of this protein, the denatured state is not so conformationally flexible that surface positions in the native state become deeply buried in the denatured state. There are some effects for the shortest linker length (ca. 10 Å), but to place that in context, such a linker puts an entire additional protein molecule at approximately the distance of the amine group on a lysine side chain.

There is another interesting observation in these data, which confirms our previous work with a single linker length. There is a presumption in the literature on excluded volume and molecular crowding that these effects will act to stabilize the native states of proteins. As we previously pointed out, this is not necessarily the case. In the data presented here, where an excluded volume effect is clearly present, the native state is less stable relative to the denatured state, not more. Although native state effects cannot be ruled out, we speculated previously (*22*) that this may be due the fact that a more compact denatured state fails to expose as much hydrophobic surface and this burial, in effect, counteracts some of the expected stability gains from lost conformational entropy. We find no reason in the data presented here to alter that view. It may be that restriction to compact denatured states does not require a large loss of conformational entropy (*42*). If this is true, and there is little difference in the hydrophobic surface exposed in the native state and in the restricted denatured state, our results are simply explained.

Lastly, the convergence of dimer denaturation behavior with that of monomers as linker length increases gives an interesting calibration for expected effects of molecular crowding. Most effects are lost or sharply attenuated by the time we reach a linker length of approximately 21 Å for $n = 3$. Admittedly, this is an attachment at only at one point on the protein surface, and the protein is not crowded on all

sides; however, it does suggest that an average separation between molecules of more than 20 Å should suffice to remove most excluded volume effects. The radius of gyration of thermally denatured nuclease has been reported as 42 Å (*47*). When assessed by small-angle X-ray scattering, both the guanidine hydrochloride denatured wild-type protein and an unstable mutant in guanidine hydrochloride have similar radii of gyration, 37.2 ± 1.2 (*48*) and 38.8 Å (*49*), respectively. Even more compact than these values is the 33 ± 1 Å radius of gyration of the wild type in 8 M urea (*50*). Taking the first value as worst case and adding half of the linker length where effects disappear implies that each protein needs a sphere, on average, of no more than 53 Å to avoid excluded volume effects. This corresponds to the situation expected at a nuclease concentration of approximately 1.7 mM or 28 mg/mL. This is a fairly high concentration, but not incredibly so. This rough calculation extrapolating from results on one protein should not be taken too seriously, but it does imply that molecular crowding effects on protein stability should indeed be observed at high protein concentrations, such as those found in the cell. However, the assumption that these effects will act to stabilize the native states of proteins relative to the denatured states should be carefully re-examined.

SUPPORTING INFORMATION AVAILABLE

Details of the synthetic procedures for each cross-linker and their characterization, the details of cross-linking reaction yields and levels of free thiol measured by Ellman's assay, and thermodynamic parameters obtained from two- and three-state fits to data obtained from guanidine hydrochloride denaturation at 100 mM NaCl. This material is available free of charge via the Internet at http://pubs.acs.org.

REFERENCES

1. Zimmerman, S. B., and Minton, A. P. (1993) Macromolecular crowding: Biochemical, biophysical, and physiological consequences. *Annu. Rev. Biophys. Biomol. Struct. 22*, 27–65.
2. Minton, A. P. (1992) Confinement as a determinant of macromolecular structure and reactivity. *Biophys. J. 63*, 1090–1100.
3. Minton, A. P. (1997) Influence of excluded volume upon macromolecular structure and associations in 'crowded' media. *Curr. Opin. Biotechnol. 8*, 65–69.
4. Ping, G., Yuan, J. M., Sun, Z., and Wei, Y. (2004) Studies of effects of macromolecular crowding and confinement on protein folding and protein stability. *J. Mol. Recognit. 17*, 433–440.
5. Ellis, R. J. (2001) Macromolecular crowding: Obvious but underappreciated. *Trends Biochem. Sci. 26*, 597–604.
6. Chebotareva, N. A., Kurganov, B. I., and Livanova, N. B. (2004) Biochemical effects of molecular crowding. *Biochemistry (Moscow, Russ. Fed.) 69*, 1239–1251.
7. Hall, D., and Minton, A. P. (2003) Macromolecular crowding: Qualitative and semiquantitative successes, quantitative challenges. *Biochim. Biophys. Acta 1649*, 127–139.
8. Despa, F., Orgill, D. P., and Lee, R. C. (2005) Molecular crowding effects on protein stability. *Ann. N.Y. Acad. Sci. 1066*, 54–66.
9. Minton, A. P. (2006) Macromolecular crowding. *Curr. Biol. 16*, R269–R271.
10. Ellis, R. J. (1997) Molecular chaperones: Avoiding the crowd. *Curr. Biol. 7*, R531–R533.
11. Zimmerman, S. B., and Trach, S. O. (1991) Estimation of macromolecule concentrations and excluded volume effects for the cytoplasm of *Escherichia coli*. *J. Mol. Biol. 222*, 599–620.
12. Dill, K. A. (1990) Dominant forces in protein folding. *Biochemistry 29*, 7133–7155.
13. Dill, K. A., and Shortle, D. (1991) Denatured states of proteins. *Annu. Rev. Biochem. 60*, 795–825.
14. Zhou, H. X., and Dill, K. A. (2001) Stabilization of proteins in confined spaces. *Biochemistry 40*, 11289–11293.
15. Minton, A. P. (2000) Effect of a concentrated "inert" macromolecular cosolute on the stability of a globular protein with respect to denaturation by heat and by chaotropes: A statistical-thermodynamic model. *Biophys. J. 78*, 101–109.
16. Minton, A. P. (2001) The influence of macromolecular crowding and macromolecular confinement on biochemical reactions in physiological media. *J. Biol. Chem. 276*, 10577–10580.
17. Zhou, Y., and Hall, C. K. (1996) Solute excluded-volume effects on the stability of globular proteins: A statistical thermodynamic theory. *Biopolymers 38*, 273–284.
18. Zhou, H. X. (2004) Protein folding and binding in confined spaces and in crowded solutions. *J. Mol. Recognit. 17*, 368–375.
19. Eggers, D. K., and Valentine, J. S. (2001) Molecular confinement influences protein structure and enhances thermal protein stability. *Protein Sci. 10*, 250–261.
20. Flaugh, S. L., and Lumb, K. J. (2001) Effects of macromolecular crowding on the intrinsically disordered proteins c-Fos and p27(Kip1). *Biomacromolecules 2*, 538–540.
21. Spencer, D. S., Xu, K., Logan, T. M., and Zhou, H. X. (2005) Effects of pH, salt, and macromolecular crowding on the stability of FK506-binding protein: An integrated experimental and theoretical study. *J. Mol. Biol. 351*, 219–232.
22. Byrne, M. P., and Stites, W. E. (1995) Chemically crosslinked protein dimers: Stability and denaturation effects. *Protein Sci. 4*, 2545–2558.
23. Byrne, M. P., Manuel, R. L., Lowe, L. G., and Stites, W. E. (1995) Energetic contribution of side chain hydrogen bonding to the stability of staphylococcal nuclease. *Biochemistry 34*, 13949–13960.
24. Riddles, P. W., Blakeley, R. L., and Zerner, B. (1983) Reassessment of Ellman's reagent. *Methods Enzymol. 91*, 49–60.
25. Schwehm, J. M., and Stites, W. E. (1998) Application of automated methods for determination of protein conformational stability. *Methods Enzymol. 295*, 150–170.
26. Stites, W. E., Byrne, M. P., Aviv, J., Kaplan, M., and Curtis, P. M. (1995) Instrumentation for automated determination of protein stability. *Anal. Biochem. 227*, 112–122.
27. Shortle, D. (2002) The expanded denatured state: An ensemble of conformations trapped in a locally encoded topological space. *Adv. Protein Chem. 62*, 1–23.
28. Baldwin, R. L. (2002) A new perspective on unfolded proteins. *Adv. Protein Chem. 62*, 361–367.
29. Bowler, B. E. (2007) Thermodynamics of protein denatured states. *Mol. BioSyst. 3*, 88–99.
30. McCarney, E. R., Kohn, J. E., and Plaxco, K. W. (2005) Is there or isn't there? The case for (and against) residual structure in chemically denatured proteins. *Crit. Rev. Biochem. Mol. Biol. 40*, 181–189.
31. Ohnishi, S., and Shortle, D. (2003) Effects of denaturants and substitutions of hydrophobic residues on backbone dynamics of denatured staphylococcal nuclease. *Protein Sci. 12*, 1530–1537.
32. Ackerman, M. S., and Shortle, D. (2002) Molecular alignment of denatured states of staphylococcal nuclease with strained polyacrylamide gels and surfactant liquid crystalline phases. *Biochemistry 41*, 3089–3095.
33. Ackerman, M. S., and Shortle, D. (2002) Robustness of the long-range structure in denatured staphylococcal nuclease to changes in amino acid sequence. *Biochemistry 41*, 13791–13797.
34. Shortle, D., and Ackerman, M. S. (2001) Persistence of native-like topology in a denatured protein in 8 M urea. *Science 293*, 487–489.
35. Carra, J. H., and Privalov, P. L. (1996) Thermodynamics of denaturation of staphylococcal nuclease mutants: An intermediate state in protein folding. *FASEB J. 10*, 67–74.
36. Eftink, M. R., Ionescu, R., Ramsay, G. D., Wong, C. Y., Wu, J. Q., and Maki, A. H. (1996) Thermodynamics of the unfolding and spectroscopic properties of the V66W mutant of staphylococcal nuclease and its 1−136 fragment. *Biochemistry 35*, 8084–8094.
37. Ionescu, R. M., and Eftink, M. R. (1997) Global analysis of the acid-induced and urea-induced unfolding of staphylococcal nuclease and two of its variants. *Biochemistry 36*, 1129–1140.
38. Gittis, A. G., Stites, W. E., and Lattman, E. E. (1993) The phase transition between a compact denatured state and a random coil state in staphylococcal nuclease is first-order. *J. Mol. Biol. 232*, 718–724.
39. Nishimura, C., Riley, R., Eastman, P., and Fink, A. L. (2000) Fluorescence energy transfer indicates similar transient and equilibrium intermediates in staphylococcal nuclease folding. *J. Mol. Biol. 299*, 1133–1146.

40. Seemann, H., Winter, R., and Royer, C. A. (2001) Volume, expansivity and isothermal compressibility changes associated with temperature and pressure unfolding of staphylococcal nuclease. *J. Mol. Biol. 307*, 1091–1102.
41. Paliwal, A., Asthagiri, D., Bossev, D. P., and Paulaitis, M. E. (2004) Pressure denaturation of staphylococcal nuclease studied by neutron small-angle scattering and molecular simulation. *Biophys. J. 87*, 3479–3492.
42. Goldenberg, D. P. (2003) Computational simulation of the statistical properties of unfolded proteins. *J. Mol. Biol. 326*, 1615–1633.
43. Pessela, B. C., Mateo, C., Carrascosa, A. V., Vian, A., Garcia, J. L., Rivas, G., Alfonso, C., Guisan, J. M., and Fernandez-Lafuente, R. (2003) One-step purification, covalent immobilization, and additional stabilization of a thermophilic poly-His-tagged β-galactosidase from *Thermus* sp. strain T2 by using novel heterofunctional chelate-epoxy Sepabeads. *Biomacromolecules 4*, 107–113.
44. Burteau, N., Burton, S., and Crichton, R. R. (1989) Stabilisation and immobilisation of penicillin amidase. *FEBS Lett. 258*, 185–189.
45. Ahmad, S., Anwar, A., and Saleemuddin, M. (2001) Immobilization and stabilization of invertase on *Cajanus cajan* lectin support. *Bioresour. Technol. 79*, 121–127.
46. Lopez-Gallego, F., Montes, T., Fuentes, M., Alonso, N., Grazu, V., Betancor, L., Guisan, J. M., and Fernandez-Lafuente, R. (2005) Improved stabilization of chemically aminated enzymes via multipoint covalent attachment on glyoxyl supports. *J. Biotechnol. 116*, 1–10.
47. Panick, G., Malessa, R., Winter, R., Rapp, G., Frye, K. J., and Royer, C. A. (1998) Structural characterization of the pressure-denatured state and unfolding/refolding kinetics of staphylococcal nuclease by synchrotron small-angle X-ray scattering and Fourier-transform infrared spectroscopy. *J. Mol. Biol. 275*, 389–402.
48. Kohn, J. E., Millett, I. S., Jacob, J., Zagrovic, B., Dillon, T. M., Cingel, N., Dothager, R. S., Seifert, S., Thiyagarajan, P., Sosnick, T. R., Hasan, M. Z., Pande, V. S., Ruczinski, I., Doniach, S., and Plaxco, K. W. (2004) Random-coil behavior and the dimensions of chemically unfolded proteins. *Proc. Natl. Acad. Sci. U.S.A. 101*, 12491–12496.
49. Nishimura, C., Uversky, V. N., and Fink, A. L. (2001) Effect of salts on the stability and folding of staphylococcal nuclease. *Biochemistry 40*, 2113–2128.
50. Flanagan, J. M., Kataoka, M., Fujisawa, T., and Engelman, D. M. (1993) Mutations can cause large changes in the conformation of a denatured protein. *Biochemistry 32*, 10359–10370.

BI800297J